Parametric adaptive control of single-rod electrohydraulic system with block-strict-feedback model

DOI:
10.1016/j.cub.2019.08.012

Document Version
Accepted author manuscript

Parametric Adaptive Control of Single-rod Electrohydraulic System with Block-Strict-Feedback Model ⋆

Qing Guo[ab c], Zongyu Zuo [d], Zhengtao Ding [e],

[a] *School of Aeronautics and Astronautics, University of Electronic Science and Technology of China, Chengdu, China*

[b] *State Key Laboratory of Fluid Power and Mechatronic Systems, Zhejiang University, Hangzhou, China*

[c] *Aircraft Swarm Intelligent Sensing and Cooperative Control Key Laboratory of Sichuan Province, Chengdu, China*

[d] *Seventh Research Division, and Science and Technology on Aircraft Control Laboratory, Beihang University, Beijing, China*

[e] *Control Systems Centre, Department of Electrical and Electronic Engineering, University of Manchester, Manchester, U.K.*

Abstract

To address the universal single-rod electrohydraulic system (EHS), a block-strict-feedback model is constructed for the position control loop design. Different from the previous strict-feedback controllers used in EHS, the proposed controller avoids the model order-reduction problem and relaxes the strict-feedback model assumption for the single-rod EHS encountered by the existing results. Hence, all the dynamic physical states of single-rod EHS are directly used in control design. Since the hydraulic parametric uncertainties and the external load would degrade the output tracking performance of EHS, an adaptive control is proposed to guarantee all system states globally and uniformly bounded with parameter adaptation. The constraint holding technique called prescribed performance constraint (PPC) is adopted to improve the output response and to achieve a desirable performance. The effectiveness of the proposed controller is demonstrated by a comparison with the strict-feedback controller via both simulation and experiments.

Key words: Single-rod electrohydraulic system; Parametric adaptive control; Block-strict-feedback control; Prescribed performance constraint.

1 Introduction

Electrohydraulic systems are widely used in mechatronic engineering as they have a superior load efficiency. However, due to unknown viscous damping, load stiffness, variations in control fluid volumes, physical characteristics of valve, bulk modulus and oil temperature variations existed in EHS [12], the high-quality dynamic performance of EHS cannot always be maintained. Furthermore, the external loads of EHS such as the driving forces and the torques of mechanical plant are unknown disturbances. To address these two problems, Yao [3] proposes a robust adaptive control to estimate the unknown parameters and the load disturbance with smooth projection [18], [20]. As mentioned in [3], there exists an internal dynamics in single-rod hydraulic actuator, due to the pressure dynamics determined by two chambers' equations, which cannot be simplified as the load pressure dynamics of the double-rod hydraulic actuator. Thus, the system stability and performance of the single-rod EHS need to be rigorously identified to disclose the essential difference from the double-rod EHS. Inspired by these consideration, this paper establishes a model of the single-rod EHS in the block-strict-feedback form [9], instead of the pure-feedback form, which eliminates the strict-feedback form assumption required by the model-reduction method.

In lots of previous work, for the convenience of control design, the single-rod EHS model is written in a strict-feedback form by model order-reduction, such as the

⋆ This work was supported by National Natural Science Foundation of China under Grants 51775089 , 61673034 and 61305092, Sichuan Science and Technology Program (2018JY0565), and Open Foundation of the State Key Laboratory of Fluid Power and Mechatronic Systems (GZKF-201515). This paper was not presented at any IFAC meeting. Corresponding author: Zongyu Zuo.

Email addresses: guoqinguestc@uestc.edu.cn (Qing Guo[ab]), zzybobby@buaa.edu.cn (Zongyu Zuo), zhengtao.ding@manchester.ac.uk (Zhengtao Ding).

work due to Guan [6] and Ahn [1]. Meanwhile, to address hydraulic parametric uncertainties, some advanced control methods have been utilized, such as robust H_∞ control [13], output regulation control [16], and parametric adaptive control [1], [22]. Parametric uncertainties are also considered in the hydraulic clutch actuator of Automated Manual Transmissions [5]. On the other hand, to suppress the external load in EHS, Kim and Won [8], [19] proposed a high-gain disturbance observer to compensate the unknown external load with guaranteed position tracking accuracy. However, to the authors' best knowledge, adaptive controller and disturbance observer designs used in EHS are based on the strict-feedback model of double-rod actuator and equivalent strict-feedback form of single-rod actuator. Thus, this study focuses on the model construction of a class of universal single-rod EHS and proposes a block-strict-feedback controller by taking into account parametric uncertainties and external load disturbances.

Inspired by previous results on the pure-feedback and block-strict-feedback nonlinear systems [10], [11], a parametric adaptive control is studied for a generic single-rod EHS based on its original model. Hence, the main contributions of this paper are twofold:

(i) Different from the model order-reduction solution in [3] and [6], this paper provides a block-strict-feedback form for the single-rod EHS. Via this formulation, the original model of the single-rod EHS is directly used in control design such that the model order-reduction is avoided. Thus, the proposed controller is more general than the ones given in the existing literature. Furthermore, by using this new block-strict-feedback model, the control performance of the single-rod EHS is better than that by using the strict-feedback model in single-rod EHS.

(ii) Without relying on the projection operator employed in [3], [6] and [21], the unknown bound of the external load and the unknown hydraulic parameters are estimated online by adaptive laws, which are in a continuous convergent function form. By introducing the prescribed performance constraint, the output position constraint is restricted in a desired accuracy. Furthermore, the adversarial impact due to parametric uncertainties and load disturbances is overcome by the proposed controller, which are verified via the single-rod EHS experimental bench.

2 Plant Description

2.1 Single-rod EHS

The single-rod EHS is comprised by a servo valve, a single-rod cylinder, a fixed displacement pump, a motor, and a relief valve as shown in Fig. 1. The external load on this EHS is a general disturbance force which drives

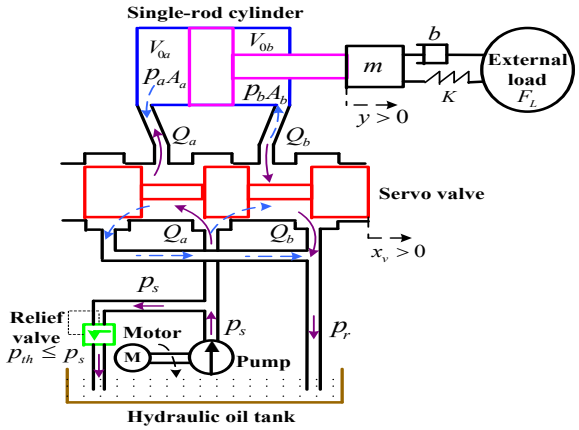

Fig. 1. The single-rod EHS control mechanism

the motion of mechanical plant. The pump is driven by the motor and outputs the supply pressure p_s, and the pressure threshold of the relief valve is often set as $p_{th} \le p_s$. As the spool position of the servo valve $x_v > 0$, the hydraulic oil passes the servo valve and enters the non-rod chamber of the cylinder. The forward channel flow Q_a and the cylinder pressure p_a are controlled by x_v. The rod chamber is connected to the return channel and the return pressure is p_r. On the other hand, the rod chamber is switched to the forward channel where the channel flow Q_b and the cylinder pressure p_b are controlled by the servo valve when $x_v < 0$. The channel flow is cut off as $x_v = 0$ where the cylinder pressure can be steadily maintained.

The channel flows $Q_i (i = a, b)$ inside two cylinder chambers are described as follows [12]:

$$\begin{aligned} Q_a &= \begin{cases} C_d w x_v \sqrt{2(p_s - p_a)/\rho} & x_v \ge 0 \\ C_d w x_v \sqrt{2(p_a - p_r)/\rho} & x_v < 0 \end{cases}, \\ Q_b &= \begin{cases} C_d w x_v \sqrt{2(p_b - p_r)/\rho} & x_v \ge 0 \\ C_d w x_v \sqrt{2(p_s - p_b)/\rho} & x_v < 0 \end{cases}, \end{aligned} \tag{1}$$

where p_a and p_b are the channel's pressures inside the two cylinder chambers, C_d and w are the discharge coefficient and the area gradient of the servo valve, x_v is the valve spool position, ρ is the density of hydraulic oil.

According to the flow conservation law, the flow-pressure equations of hydraulic cylinder are given by [13]

$$\begin{cases} A_a \dot{y} + C_{tl}(p_a - p_b) + (V_{0a} + A_a y)\dot{p}_a/\beta_e = Q_a \\ A_b \dot{y} + C_{tl}(p_a - p_b) - (V_{0b} - A_b y)\dot{p}_b/\beta_e = Q_b \end{cases}, \tag{2}$$

where y and $\dot{y}$ are the cylinder position and velocity, C_{tl} is the total leakage coefficient of the cylinder, β_e is the effective bulk modulus, A_a and A_b are the annulus areas of two cylinder chambers, V_{0a} and V_{0b} are the initial total control volumes of two chambers, respectively.

Then by the Newton's second law, the mechanical dynamic equation is described as follow [6]:

$$m\ddot{y} = p_a A_a - p_b A_b - Ky - b\dot{y} - F_L(y, \dot{y}, \ddot{y}, t), \quad (3)$$

where m is the load mass, K is load spring constant, b is the viscous damping coefficient, F_L is the external load on the EHS.

Finally, the channel flows Q_a and Q_b of the single-rod cylinder are controlled by the spool position x_v of the servo valve. Since the cut-off frequency of servo valve is far greater than the control system bandwidth, the valve dynamics can be neglected in the modeling, given by [8]

$$x_v = K_{sv} u, \quad (4)$$

where K_{sv} and u are the gain and the control voltage of the servo valve, respectively.

From (1)-(4), if the four state variables are defined as $\boldsymbol{X} = [x_1, x_2, x_3, x_4]^T = [y, \dot{y}, p_a, p_b]^T$, then the state space model of the single-rod EHS is given by

$$\begin{cases} \dot{x}_1 = x_2 \\ \dot{x}_2 = -\theta_1 x_1 - \theta_2 x_2 + g_2(x_3 A_a - x_4 A_b) + d_L \\ \dot{x}_3 = f_{31}(x_2)\theta_3 + f_{32}(\boldsymbol{X})\theta_4 + \theta_5 g_3(x_1, x_3, u)u \\ \dot{x}_4 = f_{41}(x_2)\theta_3 + f_{42}(\boldsymbol{X})\theta_4 + \theta_5 g_4(x_1, x_4, u)u \end{cases}, \quad (5)$$

where $d_L(X,t) = F_L/m$, $\theta_1 = K/m$, $\theta_2 = b/m$, $\theta_3 = \beta_e$, $\theta_4 = \beta_e C_{tl}$, $\theta_5 = \beta_e C_d w K_{sv}\sqrt{2/\rho}$, $g_2 = 1/m$ and

$$\begin{aligned} f_{31}(x_2) &= -A_a x_2/(V_{0a} + A_a x_1) \\ f_{32}(\boldsymbol{X}) &= (x_4 - x_3)/(V_{0a} + A_a x_1) \\ f_{41}(x_2) &= A_b x_2/(V_{0b} - A_b x_1) \\ f_{42}(\boldsymbol{X}) &= (x_3 - x_4)/(V_{0b} - A_b x_1) \\ g_3(x_1, x_3, u) &= [s(u)\sqrt{p_s - x_3} \\ &\quad + s(-u)\sqrt{x_3 - p_r}]/(V_{0a} + A_a x_1) \\ g_4(x_1, x_4, u) &= -[s(u)\sqrt{x_4 - p_r} \\ &\quad + s(-u)\sqrt{p_s - x_4}]/(V_{0b} - A_b x_1) \end{aligned} \quad (6)$$

Remark 1 *The function $s(u)$ in (6) is a sign function, $s(u) = 1$ for $u \geq 0$ and 0 for $u < 0$.*

Remark 2 *A new state variable $\bar{x}_3$ is introduced as $\bar{x}_3 = p_a - p_b A_b/A_a = x_3 - x_4 A_b/A_a$, then model (5) can be rewritten as*

$$\begin{cases} \dot{x}_1 = x_2 \\ \dot{x}_2 = -\theta_1 x_1 - \theta_2 x_2 + g_2 A_a \bar{x}_3 + d_L \\ \dot{\bar{x}}_3 = (f_{31}(x_2) - A_b f_{41}(x_2)/A_a)\theta_3 \\ \qquad + (f_{32}(x_1, x_3, x_4) - A_b f_{42}(x_1, x_3, x_4)/A_a)\theta_4 \\ \qquad + (g_3(x_1, x_3, u) - A_b g_4(x_1, x_4, u)/A_a)\theta_5 u \end{cases}, \quad (7)$$

where $\bar{x}_3$ represents the equivalent load pressure of the single-rod EHS. However, there are two redundant states x_3 and x_4 existed in (7). If these two cylinder chambers' pressures are assumed to be known and measurable variables, model (7) can be used in backstepping iteration. Hence, many previous works focused on this order-reduction model for the single-rod EHS, since the controllers are conveniently designed based on three scalar states in a lower triangular structure. In fact, it is not necessary to convert (5) into (7). Instead, the block-strict-feedback structure is adopted in this paper.

2.2 Double-rod EHS

The double-rod EHS can bilaterally drive the external load while the single-rod EHS drives only in a unidirectional way. The double-rod EHS has the same annulus areas of two chambers, i.e., $A_a = A_b$. Due to $p_s = p_a + p_b$, if the load pressure is defined as $p_L = p_a - p_b$, the two chambers' pressures $p_a = (p_s + p_L)/2$ and $p_b = (p_s - p_L)/2$.

Similarly, if the state vector is defined as $\boldsymbol{X} = [x_1, x_2, x_3]^T = [y, \dot{y}, p_L]^T$, then the state space model of the double-rod EHS is given by [19], [21]

$$\begin{cases} \dot{x}_1 = x_2 \\ \dot{x}_2 = -(Kx_1 + bx_2)/m + A_p x_3/m + d_L \\ \dot{x}_3 = -\dfrac{4\beta_e A_p}{V_t} x_2 - \dfrac{4\beta_e C_{tl}}{V_t} x_3 \\ \qquad + \dfrac{4\beta_e C_d w K_{sv} u}{V_t\sqrt{\rho}}\sqrt{p_s - \mathrm{sgn}(u)x_3} \end{cases}. \quad (8)$$

3 Model Analysis

Superficially, the single-rod EHS model (5) is a pure-feedback system [4] due to the control variable u embedded in the expressions of g_3 and g_4. Without loss of generality, this pure-feedback model is firstly rewritten as

$$\begin{cases} \dot{x}_1 = x_2 \\ \dot{x}_2 = -\theta_1 x_1 - \theta_2 x_2 + g_2(x_3 A_a - x_4 A_b) + d_L(\boldsymbol{X}, t) \\ \dot{\boldsymbol{\zeta}} = f_{34}(\boldsymbol{X}, u)[\theta_3, \theta_4, \theta_5]^T \end{cases}, \quad (9)$$

where $\boldsymbol{\zeta} = [x_3, x_4]^T$, $f_{34}(\boldsymbol{X}, u) = \begin{bmatrix} f_{31} & f_{32} & g_3(x_1, x_3, u)u \\ f_{41} & f_{42} & g_4(x_1, x_4, u)u \end{bmatrix}$.

Obviously, (9) is equivalent to

$$\begin{cases} \dot{x}_1 = x_2 \\ \dot{x}_2 = -\theta_1 x_1 - \theta_2 x_2 + g_2(x_3 A_a - x_4 A_b) + d_L(\boldsymbol{X}, t) \\ \dot{\boldsymbol{\zeta}} = f_{34}(\boldsymbol{X})[\theta_3, \theta_4]^T + \theta_5 \mu_{34}(\boldsymbol{X}, u^0)u \end{cases}, \quad (10)$$

where u^0 locates between zero and u, and $f_{34}(\boldsymbol{X}) = \begin{bmatrix} f_{31} & f_{32} \\ f_{41} & f_{42} \end{bmatrix}$, $\mu_{34}(X, u^0) = \begin{bmatrix} g_3(x_1, x_3, u^0) \\ g_4(x_1, x_3, u^0) \end{bmatrix}$.

Lemma 1 *The model (10) can be further transformed into a block-strict-feedback structure.*

Proof. In fact, the dynamics of x_1 and x_2 in (11) are the typical strict-feedback structure without considering the dynamics of x_3 and x_4. According to **Remark 1**, the two functions $g_3(x_1, x_3, u^0)$ and $g_4(x_1, x_4, u^0)$ can be simplified into three cases:

(i) For $u^0 > 0$, $g_3(x_1, x_3, u^0) = \sqrt{p_s - x_3}/(V_{0a} + A_a x_1)$ and $g_4(x_1, x_4, u^0) = -\sqrt{x_4 - p_r}/(V_{0b} - A_b x_1)$;

(ii) For $u^0 < 0$, $g_3(x_1, x_3, u^0) = \sqrt{x_3 - p_r}/(V_{0a} + A_a x_1)$ and $g_4(x_1, x_4, u^0) = -\sqrt{p_s - x_4}/(V_{0b} - A_b x_1)$. Thus, the mean value point u^0 is eliminated in g_3 and g_4 if $u^0 \neq 0$ in which case the EHS normally works well.

(iii) For $u^0 = 0$, $u = 0$, from (5), the single-rod EHS becomes an autonomous system. Then the spool position of servo valve is cut off to hold the chambers' pressures x_3 and x_4 with respect to the extern load $d_L(t)$. During the transition, the flow-pressure continuous equation is neglected and from (5), we have

$$\ddot{x}_1 + \theta_2 \dot{x}_1 + \theta_1 x_1 = g_2(A_a x_3 - A_b x_4) + d_L. \tag{11}$$

Since x_3, x_4, d_L and g_2 are bounded, and $\theta_1, \theta_2 > 0$, then the second-order system with respect to x_1 is input to state stable, which indicates $x_1(t) \to x_{1eq}$, where x_{1eq} is some equilibrium position. If $x_{1eq} \neq y_d(t)$, where $y_d(t)$ is the position demand, it indicates that the position control objective has not been achieved yet and the control input u will not be zero in the next transition. Then case (iii) will switch to the other two cases until $x_1 \to y_d$ is achieved by the designed controller.

Generally, the effect of the sign function $s(u)$ in different conditions can be ignored in g_3 and g_4. Therefore, the EHS model (10) can be transformed into a block-strict-feedback structure as follows:

$$\begin{cases} \dot{x}_1 = x_2 \\ \dot{x}_2 = -\theta_1 x_1 - \theta_2 x_2 + g_2(x_3 A_a - x_4 A_b) + d_L(\boldsymbol{X}, t) \\ \dot{\boldsymbol{\zeta}} = f_{34}(\boldsymbol{X})[\theta_3, \theta_4]^T + \theta_5 \mu_{34}(\boldsymbol{X}) u \end{cases}, \tag{12}$$

where $\mu_{34}(\boldsymbol{X})$ is a function of the state vector $\boldsymbol{X}$ independent of the mean value point u^0. ■

Remark 3 *Comparing (7) with (12), it can be seen that the model order-reduction assumption for the single-rod EHS is eliminated.*

Similarly, the pure-feedback model of the double-rod EHS (8) can also be transformed into the following strict-feedback form:

$$\begin{cases} \dot{x}_1 = x_2 \\ \dot{x}_2 = \bar{f}_2(x_1, x_2) + \bar{g}_2 x_3 + \Delta_2(x_1, x_2) \\ \dot{x}_3 = \bar{f}_3(x_2, x_3) + \bar{g}_3(x_3) u + \Delta_3(x_1, x_2, x_3) \end{cases}, \tag{13}$$

where $\bar{f}_2 = -\frac{\bar{K} x_1 + \bar{b} x_2}{m}$, $\bar{g}_2 = \frac{A_p}{m}$, $\bar{f}_3 = -\frac{4\bar{\beta}_e A_p}{V_t} x_2 - \frac{4\bar{\beta}_e \bar{C}_{tl}}{V_t} x_3$, $\bar{g}_3 = \frac{4\bar{\beta}_e \bar{C}_d \bar{w} K_{sv}}{V_t \sqrt{\bar{\rho}}} \sqrt{p_s - \mathrm{sgn}(u) x_3}$, Δ_2 and Δ_3 are the elements of the lumped parametric uncertainties and external load disturbance.

Assumption 1 *[17] It is assumed that $y_d(t)$ and its ith order derivatives $y_d^{(i)}(t), i = 1, 2, 3$ satisfy $|y_d(t)| \leq Y_0 < k_{c1}$ and $\left| y_d^{(i)}(t) \right| \leq Y_i$ where $Y_i (i = 0, 1, 2, 3)$ are positive constants.*

Assumption 2 *[3] Due to the physical characteristics of EHS, all the unknown parameters $\theta_i (i = 1, \ldots, 5)$ are positive and bounded, i.e., there exist the constants $\bar{\theta}_i \geq \underline{\theta}_i > 0$ such that $\underline{\theta}_i \leq \theta_i \leq \bar{\theta}_i$.*

Assumption 3 *[23] There exist an unknown constant $D \geq 0$, and a non-negative smooth function $\phi(\boldsymbol{X}, t)$: $\mathbb{R}^3 \times \mathbb{R}^+ \to \mathbb{R}$ such that $\forall \boldsymbol{X} \in \mathbb{R}^3, t \in \mathbb{R}^+$, the external load disturbance $d_L(\boldsymbol{X}, t)$ satisfies*

$$|d_L(\boldsymbol{X}, t)| \leq D\phi(\boldsymbol{X}, t). \tag{14}$$

Lemma 2 *[15] The following inequality holds for $\forall \varepsilon > 0, \eta \in \mathbb{R}$,*

$$0 \leq |\eta| - \eta \tanh(\eta/\varepsilon) \leq \kappa\varepsilon, \tag{15}$$

where κ is a constant that yields $\kappa = e^{-(\kappa+1)} \approx 0.2785$.

4 Block-strict-feedback Control with Output Constraint

4.1 Prescribed Performance Constraint

In this section, the prescribed performance constraint method will be employed to guarantee the satisfactory dynamic performance of EHS.

Firstly, the tracking error of the cylinder position is defined as $e(t) = x_1(t) - y_d(t)$. If the cylinder position x_1 is constrained in $x_1(t) \in (x_{1\min}, x_{1\max})$, and y_d is bounded by $y_{d\min} \leq y_d \leq y_{d\max}$, then we have $e_{\min} < e(t) < e_{\max}$, where $e_{\min} = x_{1\min} - y_{d\max}$, $e_{\max} = x_{1\max} - y_{d\min}$.

Definition 1 *[2] A continuous smooth function $\sigma(t) = (\sigma(0) - \sigma(\infty))e^{-\lambda t} + \sigma(\infty)$ is a weighted performance function if (I) $\sigma(t)$ is positive and monotonically decreasing; (II) $\lim_{x \to \infty} \sigma(t) = \sigma_\infty > 0$; (III) $\sigma(\infty) < \sigma(0) < 1$.*

Lemma 3 *[2] If the weighted performance function $\sigma(t)$ is designed such that $e_{\min} < e(t)/\sigma(t) < e_{\max}$, then $e(t)$ is constrained in $(e_{\min}, e_{\max})$.*

Actually, if $e(t) \geq 0$, then $e(t) \leq e(t)/\sigma(t) < e_{\max}$ due to $0 < \sigma(t) < 1$. On the other hand, if $e(t) < 0$, then $e_{\min} < e(t)/\sigma(t) < e(t)$. Thus, the tracking error $e(t)$ can be always restricted in $(e_{\min}, e_{\max})$.

By *Lemma 3*, the prescribed performance constraint (P-PC) $\sigma(t)e_{\min} < e(t) < \sigma(t)e_{\max}$ can be used to define a new state error as follow:

$$z_1(t) = T^{-1}(\frac{e(t)}{\sigma(t)}) = \ln(\frac{e_{\max}(e_{\min} - e(t)/\sigma(t))}{e_{\min}(e_{\max} - e(t)/\sigma(t))}), \quad (16)$$

where $T(\cdot)$ is a smooth function, $T^{-1}(\cdot)$ is its inverse function.

Theorem 1 *The smooth function $T(\cdot)$ is a monotonically increasing function, and yields the following properties*

$$\begin{aligned} e_{\min} < & T(z_1) < e_{\max}, \qquad T(0) = 0, \\ \lim_{z_1 \to -\infty} & T(z_1) = e_{\min}, \quad \lim_{z_1 \to +\infty} T(z_1) = e_{\max}. \end{aligned} \quad (17)$$

Proof. From (16), the inverse function of z_1 is given by

$$T(z_1) = \frac{e(t)}{\sigma(t)} = \frac{e_{\min}e_{\max}(e^{z_1} - 1)}{e_{\min}e^{z_1} - e_{\max}}. \quad (18)$$

Then the derivative of $T(z_1)$ yields

$$\frac{dT}{dz_1} = \frac{e_{\min}(e_{\min} - e_{\max})e^{z_1}}{(e_{\min}e^{z_1} - e_{\max})^2} > 0, \quad (19)$$

due to $e_{\min} < 0$ and $e_{\max} > 0$. Hence, $T(z_1)$ is a monotonically increasing function. Furthermore, due to the PPC $\sigma(t)e_{\min} < e(t) < \sigma(t)e_{\max}$ with $\sigma(t) > 0$, $e_{\min} < T(z_1) < e_{\max}$ is established. As $z_1 \to \pm\infty$, $T(z_1)$ approaches its bound $e_{\max}$ and $e_{\min}$, respectively. If $z_1 = 0$ is substituted into (18), then $T(0) = 0$. ■

4.2 Block-strict-feedback Controller Design

For single-rod EHS, its parametric adaptive control scheme with output constraint is shown in Fig. 2. The state errors of EHS $z_i (i = 1, 2, 3)$ are defined as z_1 is given in (16), $z_2 = x_2 - \alpha_1$, $\boldsymbol{z}_3 = \boldsymbol{\zeta} - \boldsymbol{\alpha}_2$, where $\boldsymbol{\zeta} = [x_3, x_4]^T$, $\alpha_i (i = 1, 2)$ are the virtual control variables. Here $\boldsymbol{z}_3$ and $\boldsymbol{\alpha}_2$ are both vectors, while z_1, z_2 and α_1 are all scalars.

Step 1: The derivative of z_1 is given by

$$\begin{aligned} \dot{z}_1(t) &= \frac{\partial T^{-1}}{\partial(e/\sigma)} \frac{d(e/\sigma)}{dt} = r(\dot{e}(t) - e\dot{\sigma}/\sigma) \\ &= r(x_2 - \dot{y}_d - e\dot{\sigma}/\sigma) \end{aligned}, \quad (20)$$

where $r = \frac{\partial T^{-1}}{\partial(e/\sigma)} \frac{1}{\sigma} = \frac{e_{\max} - e_{\min}}{(e_{\max} - e/\sigma)(e/\sigma - e_{\min})} \frac{1}{\sigma} > 0$.

If the candidate Lyapunov function is given by

$$V_1 = \frac{1}{2} z_1^2, \quad (21)$$

then its time derivative yields

$$\begin{aligned} \dot{V}_1 &= z_1 \dot{z}_1 = z_1 r(x_2 - \dot{y}_d - e\dot{\sigma}/\sigma) \\ &= z_1 r(z_2 + \alpha_1 - \dot{y}_d - e\dot{\sigma}/\sigma) \end{aligned}. \quad (22)$$

If the virtual control variable α_1 is designed as

$$\alpha_1 = \dot{y}_d + e\dot{\sigma}/\sigma - k_1 z_1 / r, \quad (23)$$

where k_1 is a positive constant, then substituting (23) into (22), $\dot{V}_1$ yields

$$\dot{V}_1 = -k_1 z_1^2 + r z_1 z_2, \quad (24)$$

where $r z_1 z_2$ will be compensated in next step.

Step 2: For simple writing, a symbol $\mu_2 = g_2[A_a, -A_b]^T$ is defined, and the time derivative of z_2 can be derived as

$$\begin{aligned} \dot{z}_2 &= \dot{x}_2 - \dot{\alpha}_1 = -\theta_1 x_1 - \theta_2 x_2 + \mu_2^T \zeta + d_L - \dot{\alpha}_1 \\ &= -\theta_1 x_1 - \theta_2 x_2 + \mu_2^T (\boldsymbol{z}_3 + \boldsymbol{\alpha}_2) - \dot{\alpha}_1 + d_L \end{aligned}. \quad (25)$$

If let $\tilde{\theta}_i = \theta_i - \hat{\theta}_i (i = 1, 2)$, $\tilde{D} = D - \hat{D}$ be the estimated errors of the corresponding unknown parameters, where $\hat{\theta}_i$ and $\hat{D}$ are the estimates of θ_i and D, respectively, then the candidate Lyapunov function is given by

$$V_2 = V_1 + \frac{1}{2} z_2^2 + \sum_{i=1}^{2} \frac{1}{2\lambda_i} \tilde{\theta}_i^2 + \frac{1}{2\lambda_D} \tilde{D}^2, \quad (26)$$

where λ_1, λ_2, λ_D are positive constants.

Thus, the time derivative of V_2 is given by

$$\begin{aligned} \dot{V}_2 =& \dot{V}_1 + z_2 \dot{z}_2 - \sum_{i=1}^{2} \frac{1}{\lambda_i} \tilde{\theta}_i \dot{\hat{\theta}}_i - \frac{1}{\lambda_D} \tilde{D} \dot{\hat{D}} \\ \leq & - k_1 z_1^2 + z_2 (r z_1 - \theta_1 x_1 - \theta_2 x_2 + \mu_2^T \boldsymbol{\alpha}_2 - \dot{\alpha}_1) \\ & + z_2 \mu_2^T \boldsymbol{z}_3 + z_2 d_L - \sum_{i=1}^{2} \frac{1}{\lambda_i} \tilde{\theta}_i \dot{\hat{\theta}}_i - \frac{1}{\lambda_D} \tilde{D} \dot{\hat{D}} \end{aligned}. \quad (27)$$

By using **Assumption 3**, **Lemma 2**, and let $\varepsilon = \varepsilon_0/D$, the following inequality holds:

$$z_2 d_L \leq z_2 D\phi \tanh(z_2\phi/\varepsilon) + \kappa D\varepsilon. \tag{28}$$

Considering the uncertain parameters $\theta_i (i = 1, 2)$ and D in (27), the parametric adaptive laws and the virtual control variable $\boldsymbol{\alpha}_2$ are designed as follows:

$$\begin{cases} \dot{\hat{\theta}}_1 = -\lambda_1 z_2 x_1 - \lambda_1\gamma_1(\hat{\theta}_1 - \theta_{10}) \\ \dot{\hat{\theta}}_2 = -\lambda_2 z_2 x_2 - \lambda_2\gamma_2(\hat{\theta}_2 - \theta_{20}) \\ \dot{\hat{D}} = \lambda_D z_2\phi \tanh(z_2\phi/\varepsilon) - \lambda_D\gamma_D(\hat{D} - D_0) \end{cases}, \tag{29}$$

$$\begin{aligned} \boldsymbol{\alpha}_2 = &- \operatorname{diag}\{\mu_2(1), \mu_2(2)\}^{-1}\{k_2 z_2 + r z_1 \\ &- \hat{\theta}_1 x_1 - \hat{\theta}_2 x_2 - \dot{\alpha}_1 + \hat{D}\phi \tanh(z_2\phi/\varepsilon)\} \end{aligned}, \tag{30}$$

where k_2, γ_1, γ_2 and γ_D are positive constants, θ_{10}, θ_{20} and D_0 are the predictive values of the corresponding parameters, $\mu_2(1) = g_2 A_a$, $\mu_2(2) = -g_2 A_b$.

Furthermore, recalling the Young's inequality, the following inequalities hold

$$\begin{aligned} &\tilde{\theta}_i(\hat{\theta}_i - \theta_{i0}) \leq -\tilde{\theta}_i^2/2 + (\theta_i - \theta_{i0})^2/2,\ i = 1, 2 \\ &\tilde{D}(\hat{D} - D_0) \leq -\tilde{D}^2/2 + (D - D_0)^2/2 \end{aligned}. \tag{31}$$

Substituting (28)-(31) into (27), $\dot{V}_2$ yields

$$\begin{aligned} &\dot{V}_2 \leq \bar{\dot{V}}_2 + z_2\mu_2^T \boldsymbol{z}_3 + \Omega_1 \\ &\bar{\dot{V}}_2 = -k_1 z_1^2 - k_2 z_2^2 - \sum_{i=1}^{2} \gamma_i \tilde{\theta}_i^2/2 - \gamma_D \tilde{D}^2/2 < 0 \end{aligned}, \tag{32}$$

where $\Omega_1 = \frac{\gamma_1(\theta_1 - \theta_{10})^2 + \gamma_2(\theta_2 - \theta_{20})^2 + (D - D_0)^2}{2} + \kappa D\varepsilon$.

Step 3: Similar to *Step 2*, the time derivative of z_3 is given by

$$\dot{\boldsymbol{z}}_3 = \dot{\boldsymbol{\zeta}} - \dot{\boldsymbol{\alpha}}_2 = f_{34}(\boldsymbol{X})[\theta_3, \theta_4]^T + \theta_5\mu_{34}(\boldsymbol{X})u - \dot{\boldsymbol{\alpha}}_2. \tag{33}$$

The candidate Lyapunov function is given by

$$V_3 = V_2 + \frac{1}{2}\boldsymbol{z}_3^T\boldsymbol{z}_3 + \sum_{i=3}^{5} \frac{1}{2\lambda_i}\tilde{\theta}_i^2, \tag{34}$$

where $\lambda_i (i = 3, 4, 5)$ are positive constants. The time derivative of V_3 is given by

$$\begin{aligned} \dot{V}_3 =& \dot{V}_2 + \boldsymbol{z}_3^T\dot{\boldsymbol{z}}_3 - \sum_{i=3}^{5} \frac{1}{\lambda_i}\tilde{\theta}_i\dot{\hat{\theta}}_i \\ \leq& \bar{\dot{V}}_2 + \boldsymbol{z}_3^T(f_{34}(\boldsymbol{X})[\theta_3, \theta_4]^T + \theta_5\mu_{34}(\boldsymbol{X}, u)u - \dot{\boldsymbol{\alpha}}_2) \cdot \\ &+ z_2\mu_2^T\boldsymbol{z}_3 - \sum_{i=3}^{5} \frac{1}{\lambda_i}\tilde{\theta}_i\dot{\hat{\theta}}_i + \Omega \end{aligned} \tag{35}$$

To this end, the parametric adaptive laws and the final control variable u can be derived as

$$\begin{cases} \dot{\hat{\theta}}_3 = \lambda_3[f_{31}, f_{32}]^T\boldsymbol{z}_3 - \lambda_3\gamma_3(\hat{\theta}_3 - \theta_{30}) \\ \dot{\hat{\theta}}_4 = \lambda_4[f_{41}, f_{42}]^T\boldsymbol{z}_3 - \lambda_4\gamma_4(\hat{\theta}_4 - \theta_{40}) \\ \dot{\hat{\theta}}_5 = \lambda_5\boldsymbol{z}_3^T\mu_{34}(\boldsymbol{X}, u)u - \lambda_5\gamma_5(\hat{\theta}_5 - \theta_{50}) \end{cases}, \tag{36}$$

$$\begin{aligned} u = &- \frac{1}{\hat{\theta}_5\boldsymbol{z}_3^T\mu_{34}(\boldsymbol{X}, u)}(k_3\boldsymbol{z}_3^T\boldsymbol{z}_3 + \boldsymbol{z}_3^T f_{34}(\boldsymbol{X})[\hat{\theta}_3, \hat{\theta}_4]^T \\ &+ z_2\mu_2^T\boldsymbol{z}_3 - \boldsymbol{z}_3^T\dot{\boldsymbol{\alpha}}_2) \end{aligned}, \tag{37}$$

where k_3, γ_3, γ_4 and γ_5 are positive constants, $\theta_{i0} (i = 3, 4, 5)$ are the initial values of the corresponding parameters.

Similarly, by using the Young's inequality, we have

$$\tilde{\theta}_i(\hat{\theta}_i - \theta_{i0}) \leq -\tilde{\theta}_i^2/2 + (\theta_i - \theta_{i0})^2/2,\ i = 3, 4, 5. \tag{38}$$

Substituting (36)-(38) into (35), $\dot{V}_3$ yields

$$\begin{aligned} \dot{V}_3 &\leq \bar{\dot{V}}_2 - k_3\boldsymbol{z}_3^T\boldsymbol{z}_3 + \sum_{i=3}^{5} \gamma_i\tilde{\theta}_i(\hat{\theta}_i - \theta_{i0}) + \Omega_1 \\ &\leq -\sum_{i=1}^{2} k_1 z_1^2 - k_3\boldsymbol{z}_3^T\boldsymbol{z}_3 - \frac{1}{2}\sum_{i=1}^{5} \gamma_i\tilde{\theta}_i^2 - \frac{1}{2}\gamma_D\tilde{D}^2 + \Omega_2 \end{aligned}, \tag{39}$$

where $\Omega_2 = \Omega_1 + \sum_{i=3}^{5} \frac{\gamma_5}{2}(\theta_i - \theta_{i0})^2$.

Theorem 2 *Consider the EHS system (5) with the output error transformation (16), the adaptive controller (37) together with the virtual control functions (23), (30), and the parametric adaptive laws (29), (36). Under **Assumptions 1-3** and **Lemmas 1-3**, for initial conditions $\boldsymbol{X}(0) \in \Omega_{\boldsymbol{X}0}$, where $\Omega_{\boldsymbol{X}0} := \{\boldsymbol{X} \in \mathbb{R}^3 : x_{1\min} < x_1(0) < x_{1\max}, p_r < x_3(0), x_4(0) < p_s\}$, there exist suitable design parameters $k_i (i = 1, 2, 3)$, $\lambda_j, \gamma_j (j = 1, \ldots, 5)$ and γ_D used in the proposed adaptive control scheme such that (i) all closed-loop signals including $x_i (i = 1, \ldots, 4)$, $\hat{\theta}_j (j = 1, \ldots, 5)$ and $\hat{D}$ are bounded; (ii)*

the output tracking error $e(t)$ is constrained in the designed PPC $\sigma(t)e_{\min} < e(t) < \sigma(t)e_{\max}$; (iii) $e(t)$ can be reduced to arbitrarily small residual set.

Proof. From (21), (26) and (34), the cascade Lyapunov function $V_3 > 0$ holds. If let $c = \min\{2k_i(i = 1,2,3), \gamma_j(j = 1,\ldots,5), \gamma_D\}$, then from (39), the time derivative of V_3 is given by

$$\dot{V}_3 \leq -cV_3 + \Omega_2. \tag{40}$$

Integrating both sides of (40), $\dot{V}_3$ yields

$$V(t) \leq V(0)e^{-ct} + \Omega_2(1 - e^{-ct})/c. \tag{41}$$

Now from (41), and letting $t \to \infty$, the errors $z_i(i = 1,2,3)$ and the parametric adaption errors $\tilde{\theta}_j$, $\tilde{D}$ converge to the bounded residual set Ω_2/c. According to **Assumption 1**, the demand position y_d and its first two derivatives $\dot{y}_d$ and $\ddot{y}_d$ are bounded, which implies from the definitions of $z_i(i = 1,2,3)$ that the system states $x_i(i = 1,\ldots,4)$ are bounded too. Furthermore, it follows from **Assumption 2** that $\hat{\theta}_j = \theta_j - \tilde{\theta}_j$ is also bounded for $j = 1,\ldots,5$. Recalling **Assumption 3**, we have that the estimate D is also bounded. Similarly, the parametric adaption $\hat{D}$ is bounded. In addition, from **Lemma 3** and the logarithm definition of z_1, the output tracking error $e(t)$ is constrained in the PPC $\sigma e_{\min} < e(t) < \sigma e_{\max}$. Finally, the residual set Ω_2/c can be reduced to arbitrarily small by the increasing control gains $k_i(i = 1,2,3)$, the adaptation gains $\gamma_j(j = 1,\ldots,5)$ and γ_D. ■

Remark 4 *[14] The control gains $k_i(i = 1,2,3)$ are regulated to obtain tradeoff between the tracking performances of EHS and the significant chatter of the control response. Furthermore, the parametric estimation gains $\lambda_i(i = 1,\ldots,5)$, λ_D, $\gamma_i(i = 1,\ldots,5)$ and γ_D have impact on the convergent velocities of parametric estimations. Too large estimation gain will degrade the transient smoothness of estimation response.*

5 Simulation

5.1 Related parameter setup

The nominal values of the hydraulic parameters $\bar{C}_d = 0.62$, $\bar{w} = 0.024$ m, $L_{\max} = 1$ m, $p_s = 40$ bar, $p_r = 2$ bar, $A_a = 2.01$ cm^2, $A_b = 1.23$ cm^2, $V_{0a} = V_{0b} = 1.01 \times 10^{-4}$ m^3, $\bar{C}_{tl} = 2.5 \times 10^{-11}$ m^3/(s·Pa), $\bar{\beta}_e = 7000$ bar, $\bar{\rho} = 850$ kg/m^3, $\bar{K} = 500$ N/m, $\bar{b} = 50$ Ns/m, $K_{sv} = 4.9 \times 10^{-7}$ m/V are fixed. The control parameters are selected as $k_1 = 500$, $k_2 = 200$ and $k_3 = 0.25$, $\lambda_1 = \lambda_2 = 50$, $\lambda_3 = 5000$, $\lambda_4 = 30$, $\lambda_5 = 1 \times 10^{-18}$, $\lambda_D = 10$, $\gamma_1 = \gamma_2 = \gamma_4 = \gamma_5 = 0.1$, $\gamma_3 = 0.001$, $\lambda_D = 0.3$, $\varepsilon = 0.01$, $x_{1\min} = -50$ mm, $x_{1\max} = 50$ mm, $y_{d\min} = -50$ mm,

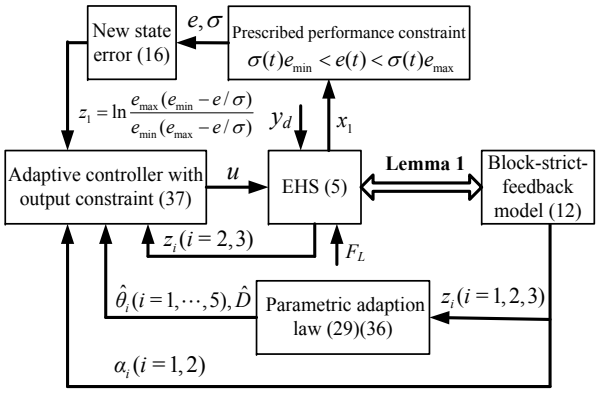

Fig. 2. The Block diagram of the parametric adaptive control scheme with output constraint

$y_{d\max} = 50$ mm, $\sigma(0) = 0.95$, $\sigma(\infty) = 0.03$, $\lambda = 2$. The initial predictive values of the hydraulic parameters are $\theta_{10} = 225$, $\theta_{20} = 20$, $D_0 = 30$, $\theta_{30} = 6.3 \times 10^8$, $\theta_{40} = 0.01925$, $\theta_{50} = 92.871$. The cylinder position demand is given by $y_d = 50\sin(\pi t)$ mm.

Subsequently, the strict-feedback controller for double-rod EHS (8) is derived as [7]

$$\begin{cases} \alpha_1 = \dot{y}_d + e\dot{\sigma}/\sigma - k_1 z_1/r \\ \alpha_2 = -(k_2 z_2 + r z_1 + \bar{f}_2 - \dot{\alpha}_1)/\bar{g}_2 \\ u = -(k_3 z_3 + \bar{f}_3 + \bar{g}_2 z_2 - \dot{\alpha}_2)/\bar{g}_3 \end{cases}, \tag{42}$$

where z_1 is given in (16), $z_2 = x_2 - \alpha_1$, $z_3 = x_3 - \alpha_2$, $\bar{f}_2$, $\bar{f}_3$, $\bar{g}_2$, $\bar{g}_3$ are shown in (13), and the gains $k_i((i = 1,2,3)$ are selected to be same in the PAC and MORC.

Likewise, the model order-reduction controller (MORC) for single-rod EHS (7) is given by

$$\begin{cases} \alpha_1 = \dot{y}_d + e\dot{\sigma}/\sigma - k_1 z_1/r \\ \alpha_2 = -(k_2 z_2 + r z_1 - \theta_{10} x_1 - \theta_{20} x_2 - \dot{\alpha}_1)/(g_2 A_a) \\ u = -[k_3 z_3 + (f_{31} - A_b f_{41}/A_a)\theta_{30} \\ \quad + (f_{32} - A_b f_{42}/A_a)\theta_{40} \\ \quad + g_2 A_a z_2 - \dot{\alpha}_2]/[(g_3 - A_b g_4/A_a)\theta_{50}] \end{cases}, \tag{43}$$

where z_1 is given in (16), $z_2 = x_2 - \alpha_1$, $z_3 = \bar{x}_3 - \alpha_2$.

5.2 Comparison results

The simulation results of the proposed parametric adaptive controller (PAC) are shown in Figs. 3-5. The tracking error of the cylinder position Δx_1 is always restricted in the prescribed performance constraint $e_{\min}\sigma(t) < e(t) < e_{\max}\sigma(t)$ and the steady stable error of Δx_1 is less than 1 mm. The control voltage u of servo valve evolves with the control saturation level $u_{\max} = \pm 10$ V. Furthermore, the chambers' pressures the two chambers pressures x_3 and x_4 never traverse the prescribed ranges $2 = p_r \leq x_3, x_4 \leq p_s = 40$ bar. In fact, the equivalent

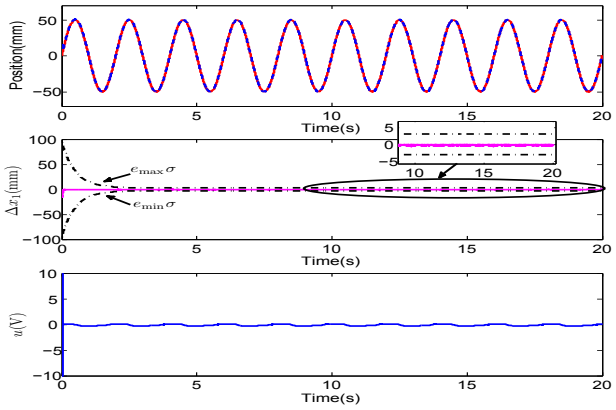

Fig. 3. The simulation results of the proposed controller (37): the red solid and the blue dashed line represent y_d and x_1 respectively, $\Delta x_1 = y_d - x_1$ is the tracking error, u is the control voltage of the servo valve.

load pressure of the single-rod cylinder p_L dynamically switches from -5 to 5 bar. The estimates of the six unknown parameters $\hat{\theta}_i (i = 1, \ldots, 5)$ and $\hat{D}$ are convergent to their respective steady values.

Then the simulation results of the controller (42) used for double-rod EHS (7) is shown in Fig. 6. Due to the strict-feedback structure of the double-rod EHS, this controller has a similar tracking position accuracy ($\Delta x_1 < 0.5$ mm) than the block-strict-feedback controller (37) does. However, the model (7) of double-rod EHS has no information about the pressures p_a and p_b due to the integration of the load pressure $p_L = p_a - p_b$. Note that the simplified load pressure of the double-rod EHS is similar to the equivalent load pressure $p_L = p_a - p_b A_b/A_a$ of the single-rod cylinder as shown in Fig. 4.

Finally, the simulation results of the model order-reduction controller (43) used for single-rod EHS (5) are shown in Fig. 7. The dynamic and steady tracking accuracy of the cylinder position is poor than that of the proposed block-strict-feedback controller as shown in Fig. 3, although the both chambers' pressures never leave their respective ranges. Indeed, the integration of the load pressure $p_L = p_a - p_b A_b/A_a$ achieves the model order-reduction which facilitates the strict-feedback control design. However, the information about the two chambers' pressures is missing in the state feedback expression, which degrades the single-rod EHS performance. Thus, the proposed block-strict-feedback controller is superior for the single-rod EHS model.

6 Experimental Verification

6.1 Single-rod EHS Bench Setup

To verify the effectiveness of the proposed parametric adaptive controller, the experimental bench of the single-rod EHS is set up as shown in Fig. 8. In fact, this

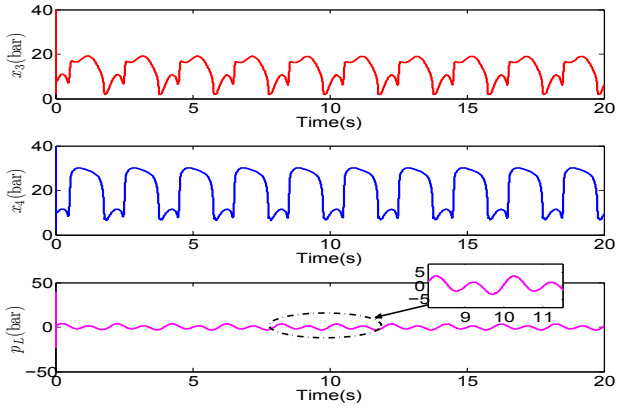

Fig. 4. The simulation results of the proposed controller (37): x_3 and x_4 are two chambers' pressures, $p_L = x_3 - x_4 A_b/A_a$ is the equivalent load pressure of the single-rod cylinder.

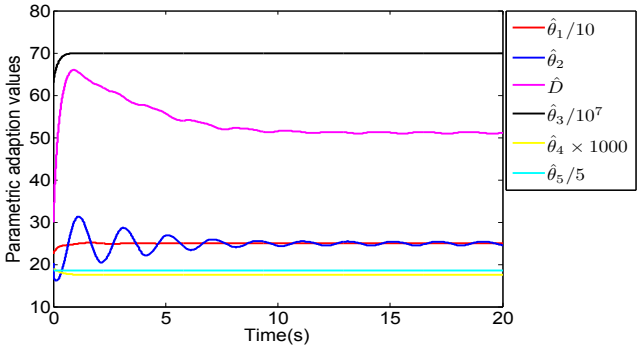

Fig. 5. The estimates of the six unknown parameters by (29) and (36).

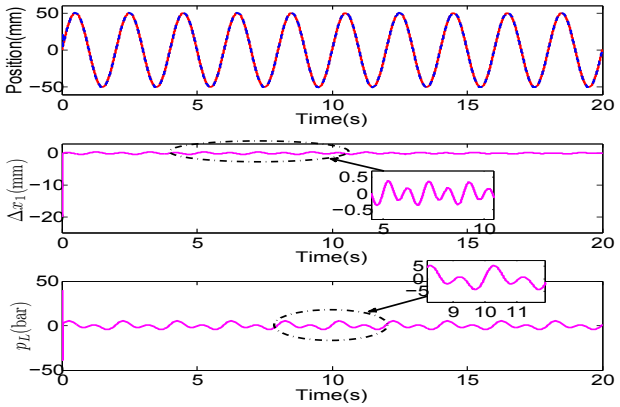

Fig. 6. The simulation results of the strict-feedback controller (42) for double-rod EHS (8): p_L is the load pressure of the double-rod cylinder.

EHS is considered to be an actuator to drive the joint motion of one manipulator. The servo valve (Brand: FF-102/03021T240) and the hydraulic cylinder (Brand: UG1511R25/16-80) are powered by a small pump station (Brand: HY-36CC-01/11kw). The cylinder position y is measured by a displacement transducer (Brand: JHQ-GA-40), and two chambers' pressures p_a, p_b are

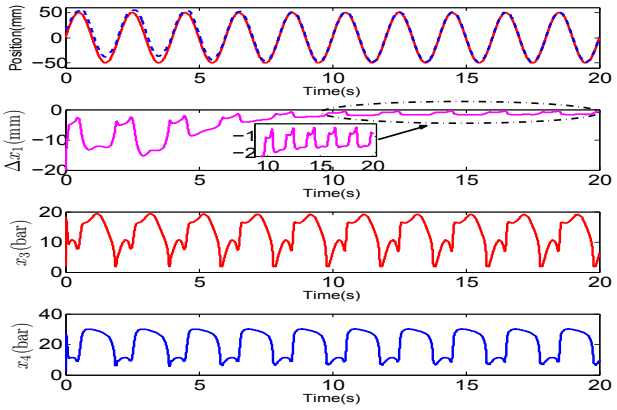

Fig. 7. The simulation results of the model order-reduction controller (43) for single-rod EHS (5): x_3 and x_4 are two chambers' pressures of the single-rod cylinder.

measured by a pressure transducer (Brand: BD-Sensors-DMP-331). The external load is generated by the driven force of the manipulator. In this study, only the forearm joint of the manipulator is controlled by the corresponding servo valve, the other joint is fixed.

The system feedback signals $(y, \dot{y}, p_a, p_b)$ are sampled by an NI card (Brand: PCI-6221). After the control algorithm is designed and compiled in MATLAB/Simulink tool in a host PC, the algorithm code is downloaded in a target computer by the driven instructions "xpcexplr". The interval of the whole algorithm execution should be appropriately chosen to guarantee that the data sampling and the control algorithm can be completed in each interval. Here, the control algorithm interval is 1 ms. As the control voltage u is returned to the NI card, the servo valve is driven to throttle two cylinder chambers' flows Q_a and Q_b supplied by the pump station. Then the joint motion of the robotic manipulator will be driven by the EHS.

The control parameters are selected as $k_1 = 200$, $k_2 = 70$ and $k_3 = 2$, $\lambda_1 = \lambda_2 = 60$, $\lambda_3 = 5000$, $\lambda_4 = 1000$, $\lambda_5 = 1 \times 10^{-16}$, $\lambda_D = 20$, $\gamma_1 = \gamma_2 = 0.02$, $\gamma_3 = 0.001$, $\gamma_4 = 1$, $\gamma_5 = 0.05$, $\lambda_D = 0.1$. The initial values of the hydraulic parameters are the same as the values used in the simulation. Taking the mechanical constraint of the cylinder displacement into account, the cylinder position demands are selected as $y_d = 30\sin(\pi t) + 25$ mm and $y_d = 30\sin(2\pi t) + 25$ mm.

6.2 Experiment results

The model order-reduction controller (MORC) directly utilized the nominal parameters of the EHS in backstepping iteration. Hence, for the sinusoidal demand $y_d = 30\sin(\pi t) + 25$ mm, the tracking performance of the MORC ($|\Delta x_1| < 4$ mm) is poor than the parametric adaptive controller (PAC) ($|\Delta x_1| < 1.5$ mm) as shown in Fig. 9. In practice, the hydraulic nominal parameters used in MORC may deviate from their true values in different working condition, which would lead to degradation of the closed-loop performance. In the proposed PAC, online parameter adaptation laws, as shown in Fig. 10, are used to counteract the model parametric uncertainties, which greatly improves the tracking performance. To further show the robustness of the PAC, the sinusoidal frequency is increased to 1 Hz and the experiment results are shown in Fig. 11. The PAC achieves better tracking performance than the MORC, which demonstrates the superiority of the PAC in dealing with the hydraulic parametric uncertainties and unknown external load encountered by the single-rod EHS. In practice, the cylinder pressure has more measured sensitive than the signals of cylinder position and velocity. Hence, in the presence of many hydraulic uncertainties and unknown external load, the proposed PAC used the direct two cylinder pressures has advantage for the uncertainty and disturbance compensation than the MORC used the equivalent load pressure in single-rod EHS.

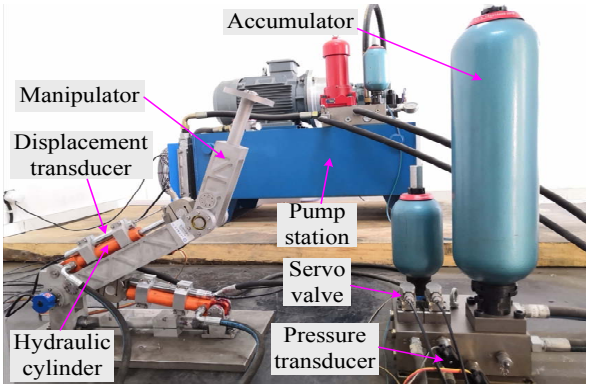

Fig. 8. The experimental bench of single-rod EHS

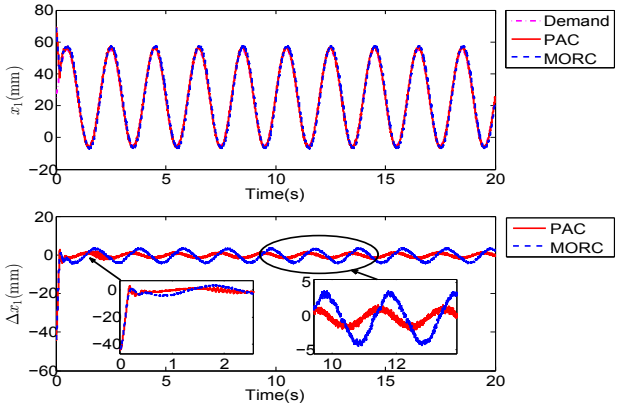

Fig. 9. The comparative experimental results: $y_d = 30\sin(\pi t) + 25$ mm.

7 Conclusion

In this paper, a block-strict-feedback control has been developed for the universal single-rod EHS to improve

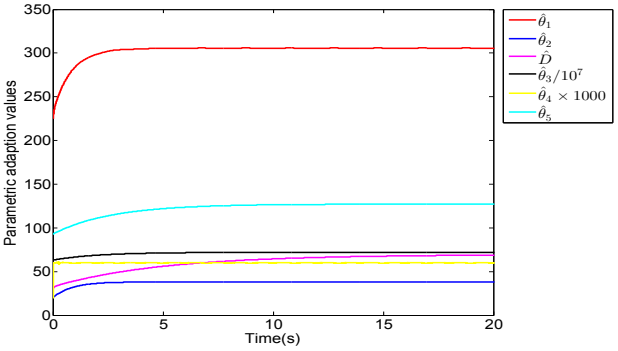

Fig. 10. The six parametric estimates in experiment.

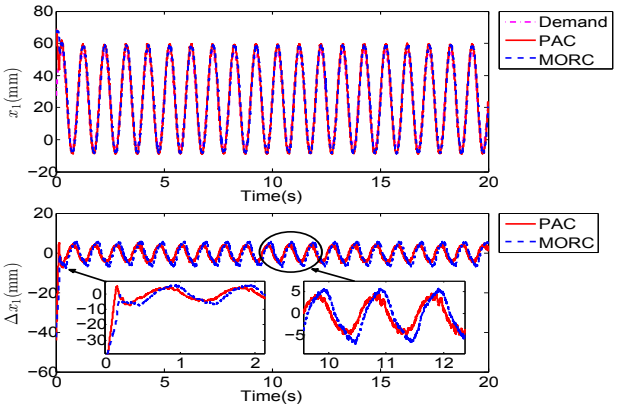

Fig. 11. The comparative experimental results: $y_d = 30\sin(2\pi t) + 25$ mm.

the dynamic and steady performance in the presence of hydraulic parametric uncertainties and unknown external load. By employing the parametric adaptive control with PPC technique, all the signals of the single-rod EHS are uniformly bounded and the tracking error of the cylinder position converges to a small compact set without violating the constraints. Meanwhile, the hydraulic parametric uncertainties and unknown external load are handled by the parametric adaptation law. Finally, the effectiveness of the proposed controller is illustrated through both simulation and experiments.

References

[1] K. K. Ahn, N. C. N. Doan, and M. Jin. Adaptive backstepping control of an electrohydraulic actuator. *IEEE/ASME Trans. Mechatronics*, 19:987–995, 2014.

[2] C. P. Bechlioulis and G. A. Rovithakis. Adaptive control with guaranteed transient and steady state tracking error bounds for strict feedback systems. *Automatica*, 45:532–538, 2009.

[3] B.Yao, F. Bu, J. Reedy, and G. T. C. Chiu. Adaptive robust motion control of single-rod hydraulic actuators theory and experiments. *IEEE/ASME Trans. Mechatronics*, 5:79–91, 2000.

[4] S. S. Ge and C. Wang. Adaptive nn control of uncertain nonlinear purefeedback systems. *Automatica*, 38:671–682, 2002.

[5] L. Glielmo, L. Iannelli, V. Vacca, and F. Vasca. Gearshift control for automated manual transmissions. *IEEE/ASME Trans. Mechatronics*, 11:17–26, 2006.

[6] C. Guan and S. Pan. Nonlinear adaptive robust control of single-rod electro-hydraulic actuator with unknown nonlinear parameters. *IEEE Trans. Control Syst. Technol.*, 16:434–445, 2008.

[7] Q. Guo, Y. Liu, D. Jiang, Q. Wang, W. Xiong, J. Liu, and X. Li. Prescribed performance constraint regulation of electrohydraulic control based on backstepping with ddynamic surface. *Appl. Sci.*, 8, 2018.

[8] W. Kim, D. Shin, D. Won, and C. C. Chung. Disturbance-observer-based position tracking controller in the presence of biased sinusoidal disturbance for electrohydraulic actuators. *IEEE Trans. Control Syst. Technol.*, 21:2290–2298, 2013.

[9] Miroslav Krstic, Ioannis Kanellakopoulos, and Peta V Kokotovic. *Nonlinear and Adaptive Control Design*. John Wiley & Sons, New York, NY, USA, 1995.

[10] Y. Li, S. Tong, and T. Li. Adaptive fuzzy output feedback dynamic surface control of interconnected nonlinear pure-feedback systems. *IEEE Trans. Cybern.*, 45:138–149, 2015.

[11] Y. Liu and S. Tong. Barrier lyapunov functions-based adaptive control for a class of nonlinear pure-feedback systems with full state constraints. *Automatica*, 64:70–75, 2016.

[12] H. Merritt. *Hydraulic control systems*. John Wiley & Sons, New York, 1967.

[13] V. Milić, Ž. Šitum, and M. Essert. Robust H_∞ position control synthesis of an electro-hydraulic servo system. *ISA Trans.*, 49:535–542, 2010.

[14] J. Na, Y. Li, Y. Huang, G.Gao, and Q. Chen. Output feedback control of uncertain hydraulic servo systems. *IEEE Trans. Ind. Electron.*, 67:490–500, 2020.

[15] M. M. Polycarpou and P. A. Ioannou. A robust adaptive nonlinear control design. *Automatica*, 32:423–427, 1996.

[16] X. Song, Y. Wang, and Z. Sun. Robust stabilizer design for linear time-varying internal model based output regulation and its application to an electro hydraulic system. *Automatica*, 50:1128–1134, 2014.

[17] K. P. Tee, S. S. Ge, and E. H. Tay. Barrier lyapunov functions for the control of output-constrained nonlinear systems. *Automatica*, 45:918–927, 2009.

[18] A. R. Teel. Adaptive tracking with robust stability. In *Proc. 32nd Conference on Decision and Control*, pages 570–575, Dec 1993.

[19] D. Won, W. Kim, D. Shin, and C. C. Chung. High-gain disturbance observer-based backstepping control with output tracking error constraint for electro-hydraulic systems. *IEEE Trans. Control Syst. Technol.*, 23:787–795, 2015.

[20] B. Yao and M. Tomizuka. Adaptive robust control of siso nonlinear systems in a semi-strict feedback form. *Automatica*, 33:893–900, 1997.

[21] J. Yao, W. Deng, and W. Sun. Precision motion control for electro-hydraulic servo systems with noise alleviation: a desired compensation adaptive approach. *IEEE/ASME Trans. Mechatronics*, 22:1859–1868, 2017.

[22] J. Yao, Z. Jiao, and D. Ma. High-accuracy tracking control of hydraulic rotary actuators with modeling uncertainties. *IEEE/ASME Trans. Mechatronics*, 19:633–641, 2014.

[23] Z. Zhang, G. Duan, and M. Hou. Robust adaptive dynamic surface control of uncertain non-linear systems with output constraints. *IET Control Theory & Appl.*, 11:110–121, 2017.